Sensors & Actuators: A. Physical 351 (2023) 114170

Contents lists available at ScienceDirect

Sensors and Actuators: A. Physical

journal homepage: www.journals.elsevier.com/sensors-and-actuators-a-physical

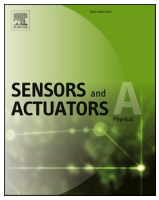

All-solid-state astringent taste sensor using polypyrrole-carbon black composite as ion-electron transducer

Moch. Rifqi Tamara [a], Danang Lelono [b], Roto Roto [c], Kuwat Triyana [a,*]

[a] Department of Physics, Universitas Gadjah Mada, Sekip Utara BLS 21, Yogyakarta, Indonesia
[b] Department of Computer Sciences dan Electronics, Universitas Gadjah Mada, Sekip Utara BLS 21, Yogyakarta, Indonesia
[c] Department of Chemistry, Universitas Gadjah Mada, Sekip Utara BLS 21, Yogyakarta, Indonesia

ARTICLE INFO

Keywords:
Lipid/polymeric membrane
Astringent sensor
Solid contact electrode
Tannic acid
Potentiometry
Polypyrrole-carbon black composite

ABSTRACT

The current development of potentiometric taste sensing still adopts a liquid-contact design. However, works on potentiometric electrodes suggest a shift towards all-solid-state electrodes (ASSE) with the advantage of solving the liquid-contact limitations. Therefore, in this study, we explore the feasibility of a taste sensor using an ASSE design by utilizing a polypyrrole-carbon black (PPy-CB) composite as an ion-electron transducer. The sensor was fabricated by depositing an astringent-selective lipid/polymeric membrane on top of a glassy carbon-modified PPy-CB electrode. Methods of characterization including scanning electron microscopy, cyclic voltammetry, impedance spectroscopy, and chronopotentiometry, were systematically performed on the as-fabricated sensor. In summary, the sensor acts similarly to the ASSE-based ion-selective electrode in that the addition of the PPy-CB layer significantly improves the stability of the sensor, owing to its high capacitance. No evidence of a water layer presents beneath the membrane and the sensor could still retain stability despite interference from O_2 and light. The fabricated sensor is highly reusable and exhibits linear behaviour toward standard astringent substance (tannic acid) in wide concentrations with a sensitivity of 17.997 mV/decade and $R^2 = 0.995$ in the wide sensing range. The proposed sensor can also respond toward gallic acid and is highly selective against interfering tastes. This demonstrates that the taste sensor can be fabricated using ASSE design, which solves some limitations of the conventional liquid-contact electrode.

1. Introduction

Taste evaluation is essential to characterize the quality of food products. A conventional way to perform such an evaluation is by employing trained human panelists. However, this method is prone to subjectivity and reproducibility owing to sensory fatigue [1]. An alternative approach is to rely on a taste sensor, which was developed by Toko et al. since 1990 [2]. The device consists of an array of electrochemical electrodes with lipid/polymer membrane (LPM) as the main sensing element. Decades of R&D by experimenting with various compositions of LPMs eventually led to specific membranes that selectively respond to the basic tastes of saltiness, sourness, sweetness, umami, bitterness, and astringency that correlated well with sensory scores [3,4].

To perform a convenient analysis, miniaturization and portability of the taste sensor are important. The developed and commercially available taste sensor electrode adopts a liquid contact design that uses a combination of an Ag/AgCl electrode and an inner filling solution as an ion-electron transducer. However, this design limits sensor miniaturization owing to the presence of the inner solution and the complexity of attaching/installing the membrane on the body of the electrode. Furthermore, the need for inner solution maintenance during storage and the inability to measure the upside-down position render this cumbersome in some applications. Attempts to miniaturize taste sensors have been proposed by introducing a gel-based electrolyte layer to replace the inner solution [5,6]. However, it has been reported that such modifications have some limitations, including deterioration of the Cl^- concentration inside the gel, sample contamination, water uptake/release, and change in gel volume which could deteriorate the electrode response [7–9].

Since the 1970 s, scientists have proposed an all-solid-state electrode (ASSE) as a potential replacement for liquid contact design, utilizing a solid material (solid contact) as an ion-electron transducer. It is fabricated by simply coating the solid contact with a membrane or equivalent

* Corresponding author.
E-mail address: triyana@ugm.ac.id (K. Triyana).

https://doi.org/10.1016/j.sna.2023.114170
Received 16 November 2022; Received in revised form 10 January 2023; Accepted 11 January 2023
Available online 13 January 2023

sensing element. Migration to ASSE-based electrodes would solve the conventional liquid-contact limitations and would benefit in many aspects including low-cost, low-material usage, adaptable measurement positioning, rapid fabrication, and easy miniaturization [10,11]. Furthermore, recent research reported that ASSE-based electrode could be fabricated in a flexible substrate [12,13], which further expand the applicability of the potentiometric sensors. To produce a robust ASSE, the solid contact material must be able to maintain a constant boundary potential without being affected by the samples. An initial ASSE, referred to as a coated wire electrode (CWE), hardly satisfies this requirement because it blocks charges from passing between ions and electrons. Its adequate response relies solely on the small double-layer capacitance between the membrane and solid substrate. Subsequently, conductive polymers such as poly(3,4-ethylenedioxythiophene):poly (styrenesulfonate) (PEDOT:PSS) [14], polypyrrole (PPy) [15], polyaniline [16], and poly(3-octylthiophene) [17] were preferred because of their redox-active nature, which is capable of directly passing charges between ions and electrons. However, further studies reported that CWE and conductive polymers could still experience potential drift owing to the tendency of water to manifest between the solid contact and membrane [18]. Furthermore, their response might be affected by external interference from soluble gases (such as O_2) [19] and light [20]. Recent studies have proposed advanced materials that can yield highly stable ASSE for use as ion-selective electrodes. Improvements in the CWE were realized by increasing the double-layer capacitance of the solid contact using hydrophobic and inert nanomaterials, including reduced graphene oxide [21,22], colloid-imprinted mesoporous carbon [23], and functionalized carbon nanotubes [9,24]. Carbon black (CB) is a promising material for use as a solid contact owing to its inert nature, high specific surface area, hydrophobicity, and low cost among carbon nanomaterials. Many studies have shown that an ASSE-based ion-selective electrode (ISE) using CB as the solid contact could significantly improve the double-layer capacitance, highly resistant to the formation of a water layer, and is almost unaffected by light, soluble gases, and even redox-active analytes [25–28]. Furthermore, CB could maintain a stable dispersion at a relatively high solid content without any functionalization [29,30], thereby maintaining its physical properties and improving the simplicity of the fabrication process.

The LPMs in the taste sensors are basically identical to some ion-selective membranes, in that the lipids used in taste sensors are lipophilic ionic salts/acids. Tetradodecylammonium bromide (TDDAB), a lipid used in commercial astringent taste sensor [31], is a quaternary ammonium salt and it has identical chemical structure with ionophore used in ISE membranes, such as tetradodecylammonium nitrate [32]. Previous work reported that TDDAB could be used as a nitrate-selective electrode, capable of achieving a near-Nernstian slope and high selectivity to interfering ions [33]. The difference between the taste sensor and ISE lies in the measurement procedure, in which the taste sensor uses a particular reference solution as a measurement baseline (mimicking the role of human saliva) to obtain potential relative and potential residues. For taste evaluation, the potential relative and potential residue signify information regarding the initial taste and aftertaste, respectively.

Based on the above description, we hypothesized that a taste sensor based on LPM fabricated using ASSE design would have a similar attribute to ISE, including the ion-electron transduction mechanism. Furthermore, the global-selective nature of the lipid-polymeric membrane could render transmembrane diffusion, which eventually causes an unstable potential if a water layer is present between the solid contact and the membrane. Finally, the transparency of the membrane and the vulnerability of gases to diffusion through the membrane could lead to instability caused by light and various non-inert gases. Therefore, in this study, we report the first attempt to investigate the stability of a taste sensor based on ASSE design. A composite of PPy and CB (PPy-CB) was selected as the solid contact. The presence of PPy should improve the stability of the ASSE owing to its high redox capacitance in tandem with the high double-layer capacitance of CB. A higher relative mass of CB from the composite was chosen to improve the overall resistance toward the formation of the water layer and the interaction of light and soluble gases during potential measurement. The investigation focused on TDDAB-loaded LPM as main sensing element that is reported to be able to selectively respond toward astringent substance. However, in this study, we mainly focused on tannic acid that is known to be used as standard for astringency and appear to be the most effective astringent than other substances. The morphology of the solid contact will be investigated using scanning electron microscopy. The solid contact capacitance of the fabricated taste sensor was characterized by using cyclic voltammetry, impedance spectroscopy, and current-reversal chronopotentiometry. Response stability was evaluated by the well-known water layer test and interference measurement in presence of O_2 and light. Finally, the stability and performance of the sensor toward astringent substance will be investigated by obtaining short- and long-term repeatability, linearity, and selectivity against interfering tastes.

2. Materials and method

2.1. Materials

PPy (doped with organic sulfonic acid anion) composites with CB at 20 wt% loading (PPy-CB, CAS#30604–81–0); tetradodecylammonium bromide ≥99% (TDDAB, CAS#14866–34–3), polyvinyl chloride (PVC, CAS#9002–86–2), bis(2-ethyhexyl) sebacate ≥97% (BEHS, CAS#122–62–3), L(+)-tartaric acid ≥99.5% (CAS#87–69–4); L-glutamic acid monosodium salt hydrate ≥99% (MSG, CAS#142–47–2), quinine monohydrochloride dihydrate ≥95% FG (Q.HCl, CAS#6119–47–7) and tetrahydrofuran ≥99% (THF, CAS#109–99–9) were purchased from Sigma-Aldrich (USA). Sodium chloride (NaCl, CAS#7647–14–5), potassium chloride (KCl, CAS#7440–09–7), potassium nitrate (KNO_3, CAS#7757–79–1), citric acid (CAS#77–92–9), tannic acid (CAS#1401–55–4), gallic acid (CAS#149–91–7), absolute ethanol (CAS#64–17–5), and N,N-dimethylformamide (DMF, CAS#68–12–2) were purchased from Merck (Germany). Glucose anhydrous (CAS#50–99–7) was purchased from Himedia (Mumbai, India). Alumina slurry (size: 0.3 μm and 0.05 μm) were purchased from Electron Microscopy Science (Hatfield, PA, USA). All solutions were prepared using distilled water.

2.2. Fabrication of all-solid-state astringent taste sensor

Fig. 1a shows the diagram of the proposed sensor fabrication. A suspension PPy-CB and lipid/polymeric membrane (LPM) cocktail were prepared in advance. The suspension was produced in 1:1 (v/v) water: DMF medium. In detail, a 25 mg PPy-CB was added in a total volume of 30 ml water:DMF. The suspension was obtained after probe-sonicated (intelligent ultrasonic generator, 19.9 kHz) the mixture for 5 min. The suspension was stored at temperatures 275–281 K while not in use. LPM cocktail was synthesized by dissolving the TDDAB (3 wt%), BEHS (64.67 wt%), and PVC (32.33 wt%) in THF (solid content of ~20 wv%). In detail, 300 mg BEHS, 150 mg PVC, and 13.9 mg TDDAB were dissolved in 2.32 ml THF. The mixture was stirred using a hotplate magnetic stirrer at a temperature of approximately 308–313 K until all solutes were completely dissolved.

The proposed sensor was fabricated by coating LPM directly on the glassy carbon (GC) modified PPy-CB electrode. The modification of GC with PPy-CB was performed by the drop-casting method. First, a 3 mm (active area) glassy carbon electrode was polished successively in alumina slurry 0.3 μm and 0.05 μm under microfibre cloth. The GC electrode was then rinsed with distilled water, ultrasonicated in distilled water for 15 min, rinsed again with distilled water, and then dried with N_2 gas. Next, 5 μl of the as-prepared PPy-CB suspension was deposited on the glassy carbon by drop-cast method every 2 h (typical drying of the suspension in the laboratory environment) for 9 cycles. This will

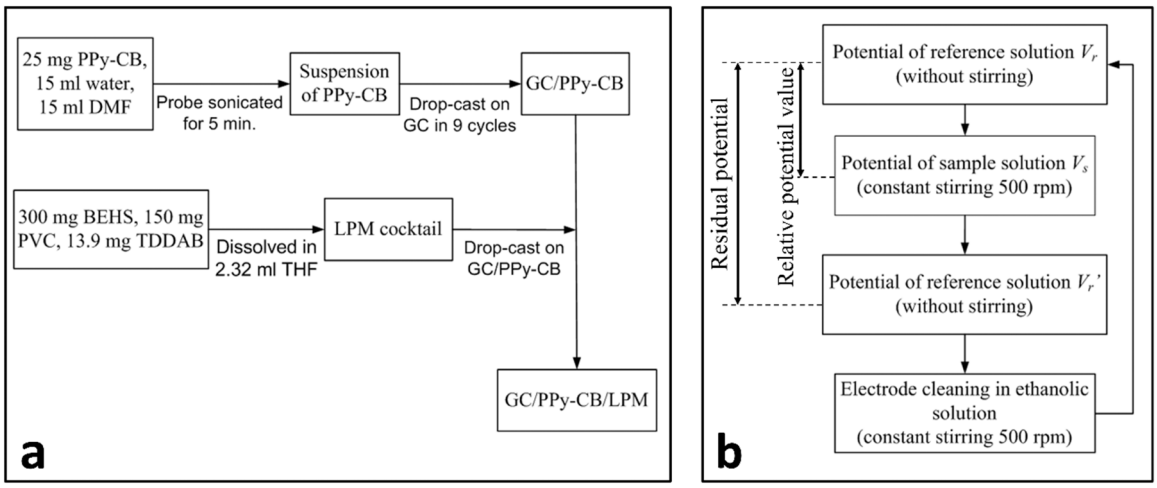

Fig. 1. Diagram of GC/PPy-CB/LPM fabrication **(a).** The proposed sensor measurement procedure **(b).**

produce GC/PPy-CB electrode which will be subject to cyclic voltammetric analysis to investigate its capacitive performance. After that, a single drop-cast of 40 μl LPM cocktail was performed on the GC/PPy-CB to obtain GC/PPy-CB/LPM electrode. Glassy carbon-coated LPM without PPy-CB as an intermediate layer (denoted as GC/LPM) was also fabricated for comparison.

2.3. Potentiometric measurement

The zero current potential of the fabricated sensor was recorded together with a double junction reference electrode (Hanna HI-5315) using ECStat Electrochemical Station. The stability of the ASSE sensor was evaluated following well-known methods, namely the water layer test and external interference study. The water layer test was performed by consecutively measuring electrode potential in the reference solution (KCl 30 mM + 0.3 mM tartaric acid), KNO_3 0.1 M solutions, then back to the reference solution. An external interference study was performed by recording the potential of the sensor in reference solution with and without the presence of O_2 and N_2 bubbling and ambient light.

Measurement of sample involved reference solution, sample solution, and cleaning solution (1:3 v/v of ethanol and HCl 0.1 M, respectively). The measurement protocol is nearly similar to the literature [34]. Fig. 1b shows the diagram of the measurement protocol. (1) Potential of the reference solution is first measured (without stirring) to obtain V_r. (2) Potential of sample solution V_s is measured until the response is saturated. Measurement was taken under constant stirring condition of 500 rpm to accelerate adsorption of astringent analyte and to improve response time. (3) Potential of the reference solution is again measured to obtain V_r'. (4) To clean adsorbed analyte in the membrane, the sensor is cleaned with the cleaning solution in constant stirring condition of 500 rpm between 30 s and 90 s. After that, the sensor is lightly rinsed with the reference solution before going back to (1) to start a new measurement. Based on the protocol, we define two output parameters of the measurement:

$$\text{Relative potential } value = V_s - V_r \quad (1)$$

$$\text{Residual potential} = V_r' - V_r \quad (2)$$

Note that the newly fabricated sensor must be conditioned in the above measurement procedure until a consistent response is obtained. Based on our data, at least 5 cycles of the above protocol were enough.

2.4. Morphological and electrochemical characterization

The structure and morphology of PPy-CB (after treatment with probe-sonication) were characterized using scanning electron microscopy (SEM, JEOL JSM-6510LA, Japan) in vacuum at 15 kV accelerated voltage after the material was gold-coated with auto fine coater (JFC-1600, Japan) in vacuum for 120 s with constant current of 20 mA. Cyclic voltammetry was performed on GC and GC/PPy-CB electrodes in reference solution at a potential ranging from −0.2 V to 0.4 V, a scan rate of 50 mV/s, 3 cycles, and a potential step of 10 mV. Impedance spectroscopy and current-reversal chronopotentiometry were performed on GC/LPM and GC/PPy-CB/LPM (as a working electrode) in a typical three-electrode system with a Hanna HI 5315 as the reference electrode, and a platinum sheet as the counter electrode. Electrochemical impedance spectroscopy (EIS) was conducted from 100 kHz to 0.05 Hz with 100 mV AC amplitude. For current-reversal chronopotentiometry, a potential was recorded for both electrodes under a continuous current of ± 1 nA each for 60 s. Prior to characterization, the electrodes were conditioned for at least 3 days in the reference solution.

3. Results and discussion

3.1. Morphological analysis

The structure and morphology of the as-deposited PPy-CB were analyzed using SEM. As shown in Fig. 2a, a magnification of × 10.000 revealed that the material has a nanomaze-like structure originating from nanoparticles that agglomerated after drying from the suspended state. In magnification of × 20.000 times, as can be seen from Fig. 2b, the size of the nanoparticle is ranging between 50 and 120 nm. The structure is quite similar to the structure of CB in other work [35]. Such a structure is expected to provide the fabricated sensor with high capacitive electrochemical behaviour owing to its high surface area.

3.2. Ion-electron transduction characterization

Performing cyclic voltammetry before the deposition of the membrane could be a fast and convenient way to characterize the solid contact. The obtained voltammograms could provide capacitive information on the solid contact, which determines the stability of the fully fabricated ASSE. In this work, cyclic voltammetry was performed for both bare and PPy-CB modified GC electrodes in a potential ranging between − 0.2 V and 0.4 V, the scan rate of 50 mV/s, 3 cycles, and the measurement step of 10 mV. As shown in Fig. 3a, both electrodes exhibited capacitive behaviour, indicated by the absence of a faradaic current. The GC-modified PPy-CB exhibited a significantly higher (ca. 2.7 times higher, measured at 0 V) capacitive current than its bare counterpart, which indicates an improved capacitance of PPy-CB on the

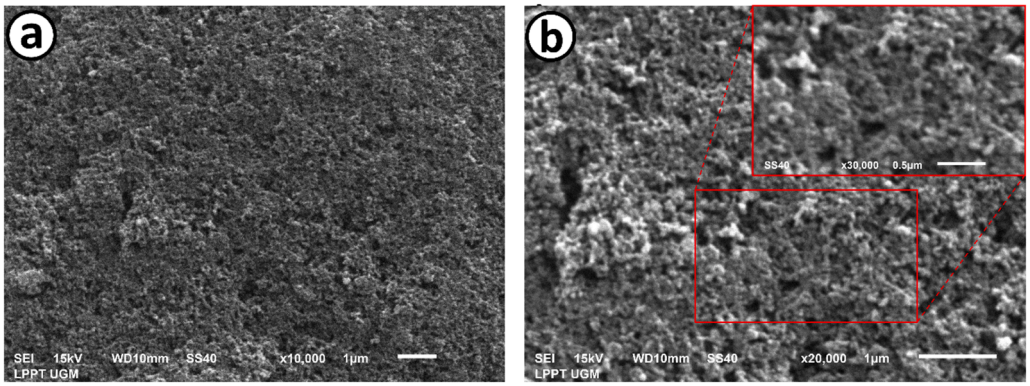

Fig. 2. SEM micrograph of PPy-CB after treatment with probe-sonication with a magnification of 10.000 **(a)** and 20.000 **(b)**. The inset shows 30.000 magnification.

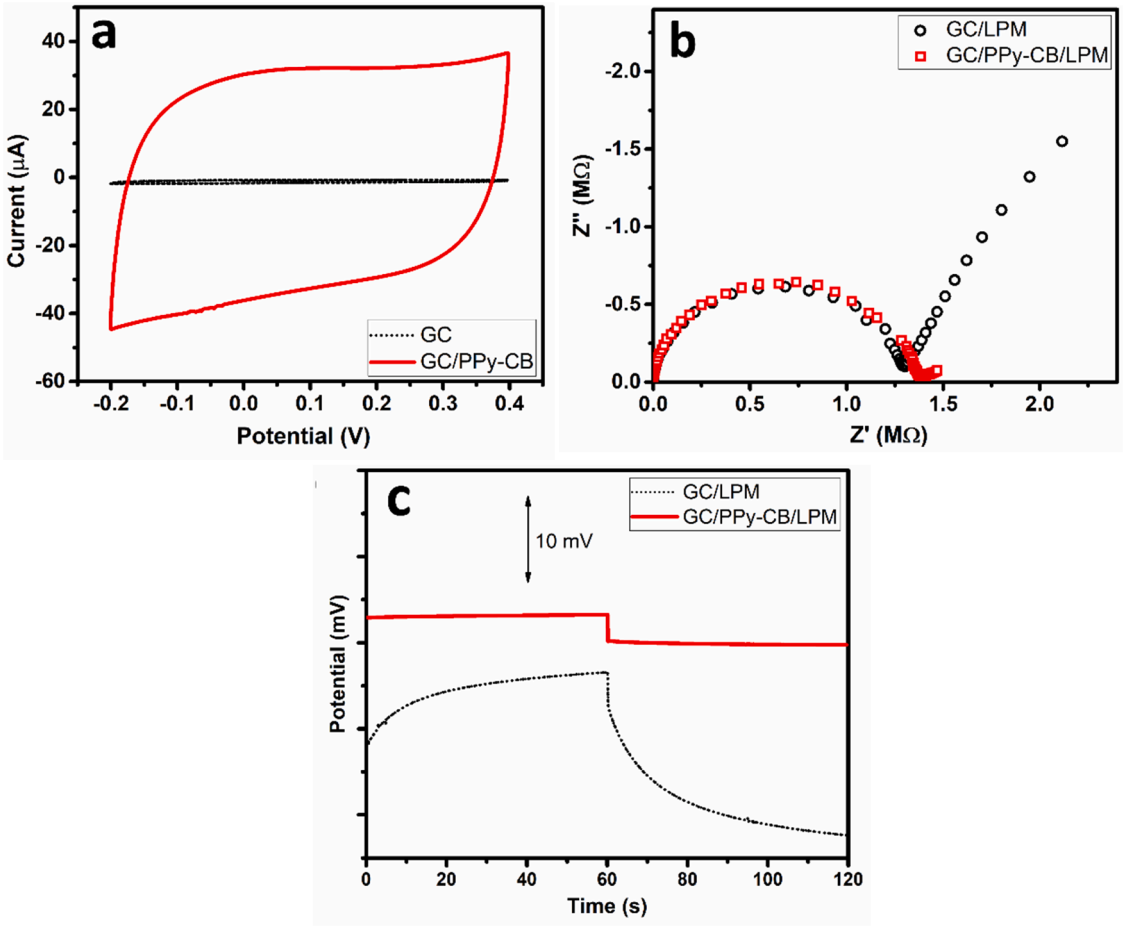

Fig. 3. Cyclic voltammogram for bare and PPy-CB modified GC electrode in reference solution with a 50 mV/s scan rate, 3 cycles, and a 10-mV measurement step **(a)**. Impedance spectra for GC/LPM and GC/PPy-CB/LPM in the reference solution with 100 mV E_{ac}, 0 V E_{dc}, and a frequency range of 100 kHz–0.05 Hz **(b)**. Chronopotentiometry was obtained for GC/LPM, and GC/PPy-CB/LPM modified glassy carbon electrodes with a constant current of ± 1 nA each for 60 s **(c)**.

surface of the electrode. The combination of the high surface area of CB and the redox-active of PPy is expected to be responsible for the improvement since high double layer and redox capacitance determines the stability of ASSE-based potentiometric electrode [10,36]. Previous works reported similar enhancements after utilizing CB as the solid contact, in the case of GC [27,37], screen-printed [38], and thermoplastic-based [39] electrodes.

Impedance measurements were performed on both GC/LPM and GC/PPy-CB/LPM from 100 kHz to 0.05 Hz at 100 mV E_{ac} and 0 V E_{dc} in the reference solution. As shown in Fig. 3b, high-frequency semicircles were observed for both sensors, which could be attributed to the bulk membrane resistance of 1.28 MΩ and 1.34 MΩ for GC/LPM and GC/PPy-CB/LPM, respectively. This slight distinction could be attributed to the uncertainty in the manual deposition of the membrane. However, a clear difference was observed in the low-frequency range, where GC/LPM exhibited a significantly larger second semicircle than that GC/PPy-CB/LPM. The low-frequency region is characteristic of solid contact beneath the membrane. The impedance spectrum for GC/PPy-CB/LPM at low frequency hardly changes, giving an absolute impedance of 1.39 MΩ at a 0.05 Hz, compared to the value obtained for GC/LPM, which is

2.62 MΩ. This indicates that the addition of PPy-CB considerably reduces the charge transfer resistance while boosting the capacitance at the solid contact layer. Similar results were observed for ion-selective electrodes with various types of solid contact layers, including multi-walled carbon nanotubes [40], porous carbon sub-micrometer spheres [41], and an inorganic buffer ionic liquid [42].

For a potentiometric sensor with ASSE design, it is necessary to investigate the sensor's capability to resist polarization using the current-reversal chronopotentiometry method. For GC/LPM and GC/PPy-CB/LPM, a constant current of + 1 nA was applied for 60 s, followed by − 1 nA for 60 s in the reference solution. As presented in Fig. 3c, a significant drift of 55.75 $\mu V/s$ (measured as slope) was observed for GC/LPM in comparison with GC/PPy-CB/LPM, which experienced only 4.25 $\mu V/s$. Moreover, an immediate high potential shift occurs for GC/LPM after the negative current is applied. On the other hand, GC/PPy-CB/LPM still retains response stability owing to the high capacitance of the PPy-CB as a solid contact. The potential drifts ($d\varphi/dt$) due to applied current i are related to the capacitance, C, of the solid contact by the well-known relation, $d\varphi/dt = i/C$. Therefore, measured capacitances are 17.9 μF and 235 μF for GC/LPM and GC/PPy-CB/LPM, respectively. This value is higher than the solid contact-based inorganic redox buffer ionic liquid (170.36 μF) [43] and reduced graphene oxide aerogel (142.86 μF) [44], also a much higher than that of the CB-based solid contact ISE [39,45].

3.3. Interference, water layer, and reversibility test

The presence of O_2 can affect the stability of an ASSE-based potentiometric sensor by forming a half-cell in the solid contact layer. Furthermore, light could also influence the boundary potential of the solid contact if it is either a conductive polymer [20] or has a semiconductor attribute with a narrow band gap [46]. Therefore, stability of the asfabricated GC/PPy-CB/LPM were studied by external interference from O_2 and light in the reference solution. As shown in Fig. 4a, there was no significant change in the sensor's response during O_2 and N_2 gas bubbling. The inset of Fig. 4a shows the effect of ambient light on the electrode response stability in reference solution. It is clearly observed that the effect of light on the electrode potential is insignificant. Although the solid contact contains PPy, a large portion of CB is expected to reduce the instability caused by the light. This observation indicates that the sensor exhibits good resistivity toward O_2 and light interference.

The water layer test is a common step to verify if the ASSE electrode could contain water sandwiched between the membrane and the solid contact, which mostly formed during the conditioning process. The presence of such a layer might provide a non-stable boundary potential caused by transmembrane diffusion of ions. An indirect method to identify such layer is by observing recorded potential from two different sample solutions containing primary and interfering ions. In this study, the method was performed on GC/LPM and GC/PPy-CB/LPM after the

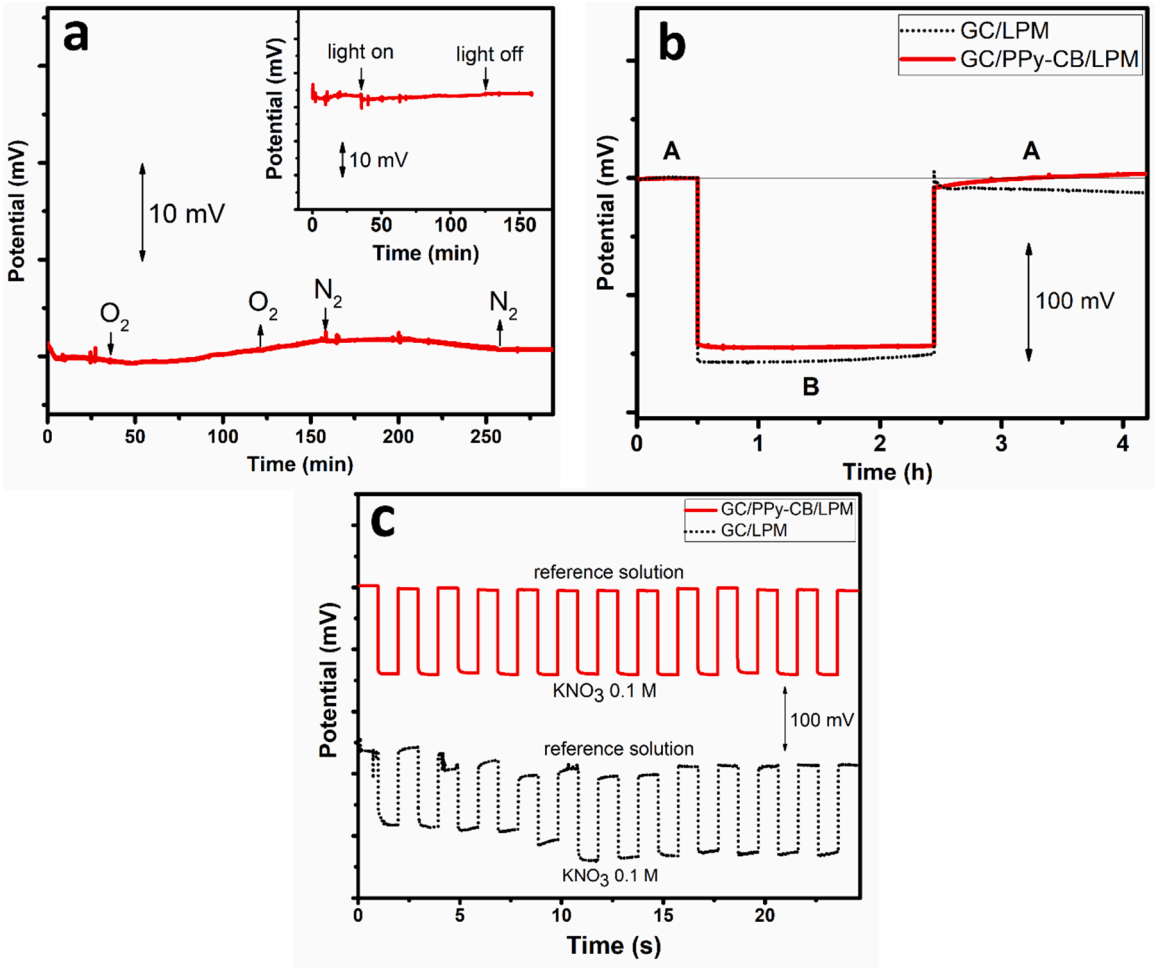

Fig. 4. Effect of O_2 on the response stability of the GC/PPy-CB/LPM. The inset shows the effect of ambient light on the stability of the GC/PPy-CB/LPM electrode. Both measurements were performed in the reference solution **(a)**. A water layer test was performed on GC/LPM and GC/PPy-CB/LPM (A = reference solution, B = 0.1 M KNO_3 solution). The potentials of all electrodes were shifted vertically so that they overlapped at the initial reference solution potential **(b)**. Reversibility response of GC/LPM and GC/PPy-CB/LPM between the reference solution and 0.1 M KNO_3 **(c)**.

sensors were conditioned in a reference solution for over one week. If a water layer is formed during conditioning, ions in the reference solution is expected to occupy the water layer. The first step was to record the potential in the reference solution (A). Because the positively charged LPM can only respond toward anions (Donan exclusion), in step two, the measurement was performed in different sample solutions that have different selectivity with anions of the reference solution, which in this case is chosen to be KNO_3. In step three, we recorded the potential back in the reference solution to observe if the recorded potential could return to the value initially recorded in step one. As shown in Fig. 4b, no significant potential drift was observed for the electrodes that were initially measured in the reference solution. Following KNO_3 0.1 M potential measurements, the response GC/LPM experienced a positive drift over time. On the other hand, the response of GC/PPy-CB/LPM was relatively stable. After placing the electrodes in the reference solution, the response of GC/PPy-CB/LPM did not immediately return to its original value of the reference solution. Instead, it slowly drifted to its original values. This might indicate that the overall composition of the ions in the membrane is altered by nitrate anions, and it takes some time to recondition back in the reference solution. In contrast, an immediate negative shift was observed for the GC/LPM electrode relative to its original value. Moreover, the electrode experienced a negative drift further away from the original line. This behaviour is very similar to previous reports in that the shift and drift might be owing to the introduction of a water layer on the solid contact, which causes instability and mechanical failure of the membrane from the GC electrode [47–49].

Reversibility tests were performed between the reference solution and KNO_3 to further emphasize the superiority of GC/PPy-CB/LPM over GC/LPM. As pointed out in the original method [18], the alternating measurement between conditioning and sample solution could not overcome the water layer problem owing to the asymmetry of drift introduced by primary and interfering ion transmembrane diffusion. Furthermore, stable reversible measurement is important for taste sensors because it uses the reference solution as a response baseline. Fig. 4c shows the reversibility response of the GC/LPM and GC/PPy-CB/LPM electrodes in the reference solution and 0.1 M KNO_3 solution in 12 successions. It can be clearly seen that the addition of PPy-CB as a solid contact provides better repeatability and reversibility as compared to the electrode that uses only bare GC as the solid contact. The inconsistency of the GC/LPM response might be caused by its vulnerability to noise, harsh conditions, and the nature of its long-term drift.

3.4. Potentiometric profile of the fabricated sensor

Selective measurement of an astringent substance, namely tannic acid, was performed using the GC/PPy-CB/LPM, by taking the residual potential as parameter. The repeatability characteristic was investigated by performing reversible measurements between the reference solution and 0.05 wt% tannic acid solution (dissolved in reference solution). As shown in Fig. 5a, a significant potential residue could be observed, indicated by the difference in V_r' and V_r. After measuring V_r', the sensor was rinsed with cleaning solution between 30 s and 90 s. Following that,

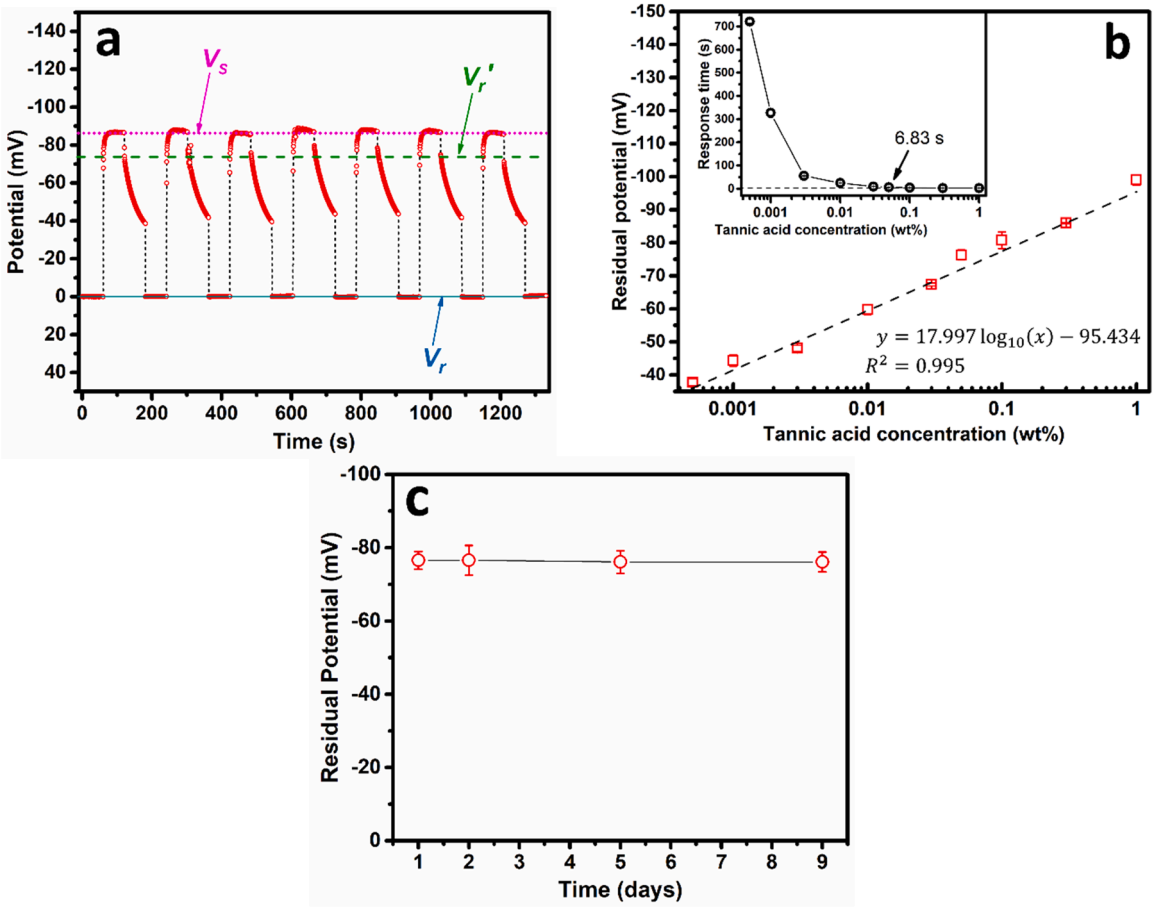

Fig. 5. Reversibility response of GC/PPy-CB/LPM measured between the reference solution and 0.05 wv% tannic acid solution (V_r = potential of the reference solution without sample residue, V_s = potential of the sample solution, $V_r^{'}$ = potential of reference solution with sample residue) (**a**). Residual potential (calculated based on Eq. 2) of GC/PPy-CB/LPM against various concentrations of tannic acid (dissolved in reference solution) ranging from 0.0005 wt% to 1 wt%. Inset shows dependency of response time toward concentrations of the tannic acid (**b**). Long-term stability of 3 replicates of GC/PPy-CB/LPM in 0.05 wt% tannic acid (dissolved in reference solution) **(c)**.

re-measurement of V_r revealed that the response instantly returned to its original value. This shows that rinsing with ethanolic solution could quickly eliminate tannic acid residue in membrane and it does not significantly affect the membrane. Also, the stable potential after the rinsing indicates that the fabricated sensor has a fast response time in the reference solution. Clearly, V_r' exhibits a potential drift over time due to desorption process of the adsorbed astringent substance in the membrane [50]. The concept of a taste sensor aims to objectively quantify the taste and aftertaste perceived by a human. Therefore, it is important to evaluate the sensor signal early in consideration of stability [34]. Despite the existence of drift, after performing 15 consecutive cycles of reversible measurement between the reference and the tannic acid solutions, the residual potential from the 0.05 wt% tannic acid (dissolved in reference solution) exhibits relatively good repeatability of -76.32 ± 1.524 mV. This value is nearly identical to the response of the taste sensor reported in previous work [5]. Fig. 5b shows the residual potential obtained toward different concentrations of tannic acid from 0.0005 wt% to 1 wt%. It can be seen that the fabricated sensor exhibits linear behaviour with a sensitivity of 17.997 mV/decade and $R^2 = 0.995$. The inset of Fig. 5b shows that the response time of the sensor depends on the concentrations of tannic acid, where the lower concentration induces higher response time. A lower concentration than 0.0005 wt% causes a further increase in response time, which makes it a bit impractical. Moreover, we observed that harsh stirring conditions for a very long time (higher than 1000 s) cause deterioration of the sensor's response. Nevertheless, the dependency of the response time (or by measuring the rate of adsorption and desorption) toward the tannic acid concentrations could potentially become a second parameter to determine astringency perception besides the residual potential. Fig. 5c shows long-term stability and reproducibility from triplicates of GC/PPy-CB/LPM. The sensors were periodically tested in 0.05 wt% tannic acid (dissolved in reference solution). While not in use, the sensors were stored in reference solution. As can be seen, the proposed sensor is reproducible and still retain original responses even after nine days of measurement.

Fig. 6a shows relative potential value response (based on Eq. 1) of the GC/PPy-CB/LPM toward KNO_3 and interfering tastes of NaCl (salty taste), citric acid (sour taste), MSG (umami taste), Q.HCl (bitter taste), and glucose (sweet taste). The LPM is positively charged owing to the lipid TDDAB, hence the sensor is sensitive toward anions (indicated by the negative trend). At a very low concentrations, the relative potential value of each substances tends to gather at ca. 175 mV above the potential of the reference solution, indicating a maximum positive-charge density generated at the membrane surface as hydrophilic group of the lipid mostly dissociate at a very dilute aqueous solution. Taking the relative potential value as the sensor output renders the sensor non-selective, as their output responses toward the analytes overlapped with others. Furthermore, the lipid TDDAB responds more sensitively toward nitrate ions in accordance with the other work which utilizes the lipid for nitrate-selective electrode [33]. Upon calculating the residual potential of each substance, no significant value is observed in various concentrations, as presented in Fig. 6b. Most of the residual potential are

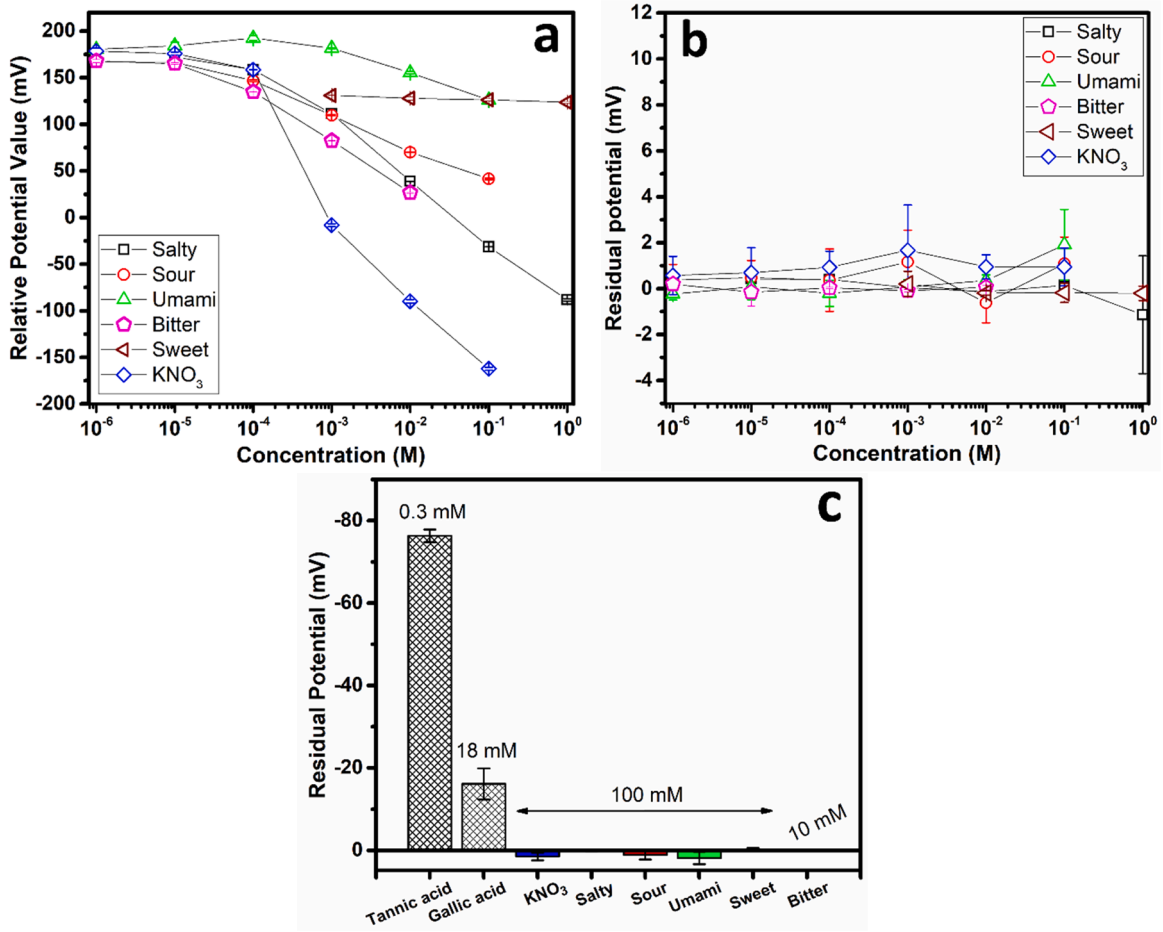

Fig. 6. Response of GC/PPy-CB/LPM toward various concentrations of the KNO_3 and interfering tastes, measured as relative potential value (calculated based on Eq. 1) **(a)**, and residual potential **(b)**. Selectivity comparison between astringent substances (tannic acid and gallic acid) and the interfering tastes **(c)**. Salty, sour, umami, bitter, and sweet correspond to NaCl, citric acid, MSG, Q.HCl, and glucose, respectively. Specifically for glucose, it is dissolved in 0.1 mM KCl to retain ionic conductivity. Each point is expressed as mean ± SD (n = 3).

positive, which seems correlated with the relative potential value in Fig. 6a. This indicates that the membrane does not adsorb or immediately desorb the interfering taste substances. Fig. 6c shows a comparison between astringent substances, which are tannic and gallic acid, with the interfering taste substances and KNO_3. Clearly, the proposed sensor has high selectivity to the astringent substances. Gallic acid is less astringent than tannic acid and is reported to be more bitter rather than astringent [51]. Tannic acid and gallic acid are known to be present in wine [52–54] and contribute to its astringency perception. However, commercially available astringent taste sensor (also use the same LPM with TDDAB lipid) is reported to be able to evaluate astringency of tannic acid, gallic acid, chlorogenic acid, caffeic acid, and epigallocatechin gallate that correlate well with sensory scores ($R^2 = 0.95$) [3]. Previous work reported that the residual potential generated by the LPM is in agreement with adsorption of epigallocathechin gallate inside the LPM at certain limit [55]. Also, recent work used the LPM-based taste sensor as standard comparison to evaluate astringency of catechins from green tea infusion [56–58].

Table 1 summarize recent works on astringency sensing. An interesting work was reported by Yeom et al. that fabricate artificial tongue by using interdigitated electrode coated with chemoresistive mucin-hydrogel. The sensor works by interacting the astringent compound with the hydrogel, transforming the gel structure and changing its chemoresistive property. The developed sensor has a similar wide sensing range to our sensor, low response time, and high accuracy. However, there was no evidence showing that the reported artificial tongue is reusable. The sensor based on lipid/polymeric membrane, however, is proven to be highly reusable. Compared to the conventional design, the proposed ASSE-based astringent sensor has a wider sensing range, low-cost, requiring very low amount of membrane material (a single sensor only needs 40 μl of the membrane cocktail), is simple to fabricate, and is easy to miniaturize. Moreover, the ASSE-based sensor has the advantage of rapid fabrication that only needs ca. 2 h to evaporate the membrane cocktail on the electrode. In comparison, the reported LPM for conventional taste sensors must evaporate the membrane cocktail for at least 3 days before it can be installed on the electrode. Furthermore, the ASSE sensor could be used in any position, which translates to its wide-range applicability. Overall, the sensing range of the proposed sensor are within human taste threshold of 30 μM [59].

3.5. Proposed mechanism

A potentiometric response can be obtained if a continuous charge transfer occurs in the system. For this, reversible charges must be passed between the electrons in the electronically conducting measuring equipment and the ionically conducting solution. In the Ag/AgCl reference electrode, ion-electron transduction is governed by a spontaneous reaction between Ag/AgCl and Cl^- ions of the internal solution. In this study, PPy-CB replaces the role of the Ag/AgCl and Cl^- in an all-solid-state taste sensor. A tentative sensing mechanism of the sensor is shown in Fig. 7. Membranes constructed from plasticized PVC with lipids could generate potential at the membrane surface owing to the dissociation of the lipid hydrophilic group and diffusion potential from charges flowing inside the membrane [34]. For the GC/LPM electrode, the membrane potential could be measured using the measuring equipment because of the double-layer capacitance formed between the electrons in the GC and the ions in the membrane, as shown in Fig. 7a. However, our data show that the capacitance generated was too small for the electrode to maintain a precise and stable potential. For GC/PPy-CB/LPM, the solid contact is composed of PPy and CB, which provide redox and double-layer capacitances, respectively. As shown in Fig. 7b, redox reactions occur between the counterion and the polymer backbone involving PPy and PPy^+, which eventually pass charges between the solid contact and electronically conducting substrate. Conversely, the high surface area of CB contributes to transduction, providing a high double-layer capacitance between the electrons and ions in the membrane. The tannic acid adsorbed onto the membrane modifies the potential generated by the membrane, reducing its surface charge density. Hence, a residual potential could be observed, which provides a unique fingerprint for the electrode as a selective astringent taste sensor.

4. Conclusions

This study presents the development of an astringent taste sensor in an ASSE design using a PPy-CB as the solid contact. The addition of the solid contact provides the electrode with a high capacitance of 235 μF and lower charge-transfer resistance than its bare counterpart, which translates well with the stability of the sensor in the reference solution. No evidence of a water layer present beneath the membrane, and the sensor could still maintain stability in the reference solution despite interference from O_2 and light. The sensor is highly reusable, providing a residual potential of -76.32 ± 1.524 mV toward a 0.05 wt% tannic acid (dissolved in reference solution) over 15 measurements, which is nearly identical to the value obtained in the literature. At various concentrations of tannic acid (0.0005–1 wt%), the sensor exhibits linear behaviour with a sensitivity of 17.997 mV/decade and $R^2 = 0.995$. Response time of the sensor depends on the concentrations of the tannic acid presents in the sample solution. The sensor can also respond to gallic acid as a minor astringent substance and highly selective against interfering taste and KNO_3. The proposed sensor has several advantages in comparison to conventional design, including wider sensing range, low-cost, requiring very low amount of membrane material (a single sensor only needs 40 μl of the membrane cocktail), rapid fabrication, and easy to miniaturize. The development of the ASSE-based taste sensor that is selective to other tastes such as saltiness, sourness, bitterness, umami, sweetness, and artificial sweetness may be subject to further investigation.

Table 1
Comparison of artificial tongue for astringency sensing reported in literature.

Sensor/Material	Measurement method	Sensing range	Response time	Selectivity, reusability	Ref.
Mucoprotein-lubricated glass	Tribometry: change in frictional force	Tannic acid (0.5–5 wt%)	N/A	N/A, yes	[60]
Interdigitated Electrode coated with chemoresistive mucin-hydrogel	Amperometry: change in ionic conductivity	Tannic acid (linear in 0.0005–1 wt%)	10 s	Yes, N/A	[59]
A specific fluorescent compound that can form complexes with catechins	Fluorescence spectroscopy: change in fluorescence intensity	EGCg[a] (linear in 0.0125–0.0738 wt%)	N/A	N/A, yes	[56]
Conventional Ag/AgCl/KCl with lipid/polymer membrane	Potentiometry: change in membrane potential caused by adsorption	Tannic acid (linear in 0.005–0.1 wt%)	N/A	Yes, yes	[4]
ASSE based on PPy-CB solid contact with lipid/polymer membrane	Potentiometry: change in membrane potential caused by adsorption	Tannic acid (linear in 0.0005–1 wt%)	Variative, ~6.83 s in tannic acid 0.05 wt% + reference solution	Yes, yes	This work

[a] EGCg = epigallocatechin-3-O-gallate

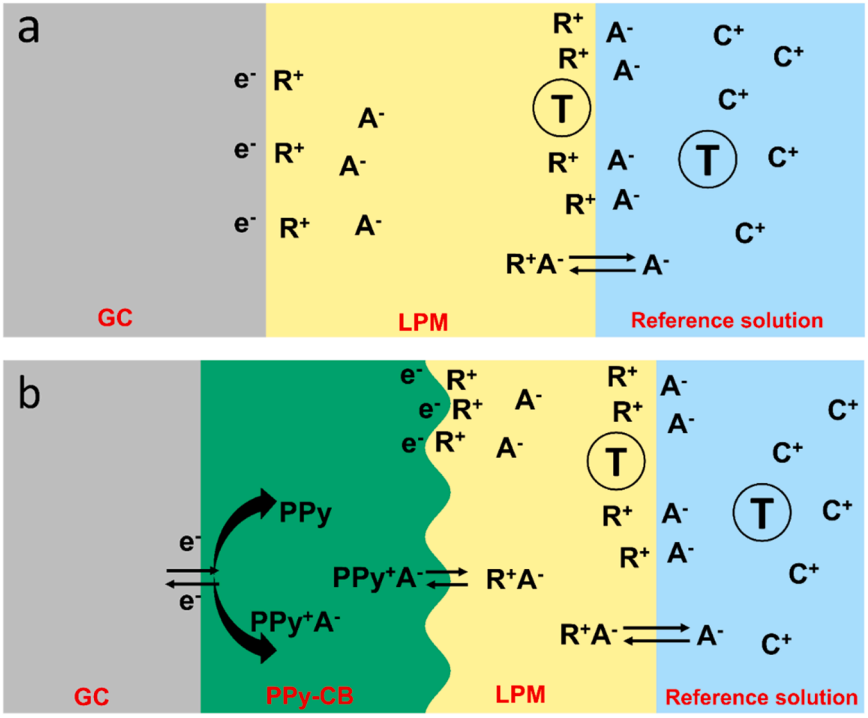

Fig. 7. Comparison between the response mechanism of GC/LPM **(a)** and GC/PPy-CB/LPM **(b)** in producing residual potential due to adsorption of tannic acid T; e^- is an electron, A^- is an anion, C^+ is a cation, R^+ is a lipid, and PPy is polypyrrole.

CRediT authorship contribution statement

Conception and design of study: K. Triyana, R. Roto, acquisition of data: M. R. Tamara, analysis and/or interpretation of data: K. Triyana, R. Roto, D. Lelono, Drafting the manuscript: M. R. Tamara, K. Triyana, revising the manuscript critically for important intellectual content: K. Triyana, R. Roto, D. Lelono, Approval of the version of the manuscript to be published (the names of all authors must be listed): M. R. Tamara, D. Lelono, R. Roto, K. Triyana.

Declaration of Competing Interest

The authors declare that they have no known competing financial interests or personal relationships that could have appeared to influence the work reported in this paper.

Data availability

Data will be made available on request.

Acknowledgment

This work was supported by the Ministry of Research, Technology and Higher Education, Republic of Indonesia through PMDSU Program (Contract No. 6825/UN1/DITLIT/DIT-LIT/PT/2021)

References

[1] M.F. Njoman, G. Nugroho, S.D.P. Chandra, Y. Permana, S. Suhadi, M. Mujiono, A. D. Hermawan, S. Sugiono, The vulnerability of human sensory evaluation and the promising senses instrumentation, Br. Food J. 119 (2017) 2145–2160, https://doi.org/10.1108/BFJ-10-2016-0505.
[2] K. Hayashi, M. Yamanaka, K. Toko, K. Yamafuji, Multichannel taste sensor using lipid membranes, Sens Actuators B Chem 2 (1990) 205–213, https://doi.org/10.1016/0925-4005(90)85006-K.
[3] Y. Kobayashi, M. Habara, H. Ikezazki, R. Chen, Y. Naito, K. Toko, Advanced taste sensors based on artificial lipids with global selectivity to basic taste qualities and high correlation to sensory scores, Sensors 10 (2010) 3411–3443, https://doi.org/10.3390/s100403411.
[4] X. Wu, K. Toko, Taste sensor with multiarray lipid/polymer membranes, TrAC - Trends Anal. Chem. 158 (2023), https://doi.org/10.1016/j.trac.2022.116874.
[5] Y. Tahara, A. Ikeda, Y. Maehara, M. Habara, K. Toko, Development and evaluation of a miniaturized taste sensor chip, Sensors 11 (2011) 9878–9886, https://doi.org/10.3390/s111009878.
[6] Y. Tahara, K. Nakashi, K. Ji, A. Ikeda, K. Toko, Development of a portable taste sensor with a lipid/polymer membrane, Sens. (Switz.) 13 (2013) 1076–1084, https://doi.org/10.3390/s130101076.
[7] S.M. Sibug-Torres, L.P. Go, E.P. Enriquez, Fabrication of a 3d-printed porous junction for Ag|AgCl|gel-KCL reference electrode, Chemosensors 8 (2020) 1–20, https://doi.org/10.3390/chemosensors8040130.
[8] J. Bobacka, Conducting polymer-based solid-state ion-selective electrodes, Electroanalysis 18 (2006) 7–18, https://doi.org/10.1002/elan.200503384.
[9] J. Kozma, S. Papp, R.E. Gyurcsányi, TEMPO-functionalized carbon nanotubes for solid-contact ion-selective electrodes with largely improved potential reproducibility and stability, Anal. Chem. 94 (2022) 8249–8257, https://doi.org/10.1021/acs.analchem.2c00395.
[10] Y. Shao, Y. Ying, J. Ping, Recent advances in solid-contact ion-selective electrodes: functional materials, transduction mechanisms, and development trends, Chem. Soc. Rev. 49 (2020) 4405–4465, https://doi.org/10.1039/c9cs00587k.
[11] D. Kałuża, A. Michalska, K. Maksymiuk, Solid-contact ion-selective electrodes paving the way for improved non-zero current sensors: a minireview, ChemElectroChem 9 (2022), https://doi.org/10.1002/celc.202100892.
[12] T. Han, T. Song, S. Gan, D. Han, J. Bobacka, L. Niu, A. Ivaska, Coulometric response of H+-selective solid-contact ion-selective electrodes and its application in flexible sensors, Chin. J. Chem. 41 (2023) 207–213, https://doi.org/10.1002/cjoc.202200500.
[13] M. Rostampour, D.J. Lawrence, Z. Hamid, J. Darensbourg, P. Calvo-Marzal, K. Y. Chumbimuni-Torres, Highly reproducible flexible ion-selective electrodes for the detection of sodium and potassium in artificial sweat, Electroanalysis (2022), https://doi.org/10.1002/elan.202200121.
[14] J. Bobacka, Potential stability of all-solid-state ion-selective electrodes using conducting polymers as ion-to-electron transducers, Anal. Chem. 71 (1999) 4932–4937, https://doi.org/10.1021/ac990497z.
[15] A. Cadogan, Z. Gao, A. Lewenstam, A. Ivaska, D. Diamond, All-Solid-state Sodium-Selective Electrode Based on a Calixarene Ionophore in a Poly(vinyl chloride) Membrane with a Polypyrrole Solid Contact, Anal. Chem. 64 (1992) 2496–2501, https://doi.org/10.1021/ac00045a007.
[16] W.-S. Han, M.-Y. Park, K.-C. Chung, D.-H. Cho, T.-K. Hong, All solid state hydrogen ion selective electrode based on a tribenzylamine neutral carrier in a poly(vinyl chloride) membrane with a poly(aniline) solid contact, Electroanalysis 13 (2001) 955–959, https://doi.org/10.1002/1521-4109(200107)13:11<955::AID-ELAN955>3.0.CO;2-5.
[17] J. Bobacka, M. McCarrick, A. Lewenstam, A. Ivaska, All solid-state poly(vinyl chloride) membrane ion-selective electrodes with poly(3-octylthiophene) solid internal contact, Analyst 119 (1994) 1985–1991, https://doi.org/10.1039/an9941901985.

[18] M. Fibbioli, W.E. Morf, M. Badertscher, N.F. De Rooij, E. Pretsch, Potential drifts of solid-contacted ion-selective electrodes due to zero-current ion fluxes through the sensor membrane, Electroanalysis 12 (2000) 1286–1292, https://doi.org/10.1002/1521-4109(200011)12:16<1286::AID-ELAN1286>3.0.CO;2-Q.
[19] M. Fibbioli, U.W. Suter, E. Pretsch, K. Bandyopadhyay, S.G. Liu, L. Echegoyen, O. Enger, F. Diederich, D. Gingery, P. Bühlmann, H. Persson, Redox-active self-assembled monolayers for solid-contact polymeric membrane ion-selective electrodes, Chem. Mater. 14 (2002) 1721–1729, https://doi.org/10.1021/cm0109589.
[20] T. Lindfors, Light sensitivity and potential stability of electrically conducting polymers commonly used in solid contact ion-selective electrodes, J. Solid State Electrochem. 13 (2009) 77–89, https://doi.org/10.1007/s10008-008-0561-z.
[21] J. Ping, Y. Wang, Y. Ying, J. Wu, Application of electrochemically reduced graphene oxide on screen-printed ion-selective electrode, Anal. Chem. 84 (2012) 3473–3479, https://doi.org/10.1021/ac203480z.
[22] J. Ping, Y. Wang, J. Wu, Y. Ying, Development of an all-solid-state potassium ion-selective electrode using graphene as the solid-contact transducer, Electrochem Commun. 13 (2011) 1529–1532, https://doi.org/10.1016/j.elecom.2011.10.018.
[23] J. Hu, X.U. Zou, A. Stein, P. Bühlmann, Ion-selective electrodes with colloid-imprinted mesoporous carbon as solid contact, Anal. Chem. 86 (2014) 7111–7118, https://doi.org/10.1021/ac501633r.
[24] S. Papp, J. Kozma, T. Lindfors, R.E. Gyurcsányi, Lipophilic multi-walled carbon nanotube-based solid contact potassium ion-selective electrodes with reproducible standard potentials. A comparative study, Electroanalysis 32 (2020) 867–873, https://doi.org/10.1002/elan.202000045.
[25] T. Ozer, Carbon composite thermoplastic electrodes integrated with mini-printed circuit board for wireless detection of calcium ions, Anal. Sci. (2022), https://doi.org/10.1007/s44211-022-00164-w.
[26] T. Ozer, C.S. Henry, All-solid-state potassium-selective sensor based on carbon black modified thermoplastic electrode, Electro Acta 404 (2022), https://doi.org/10.1016/j.electacta.2021.139762.
[27] B. Paczosa-Bator, All-solid-state selective electrodes using carbon black, Talanta 93 (2012) 424–427, https://doi.org/10.1016/j.talanta.2012.02.013.
[28] V. Mazzaracchio, A. Serani, L. Fiore, D. Moscone, F. Arduini, All-solid state ion-selective carbon black-modified printed electrode for sodium detection in sweat, Electro Acta 394 (2021), https://doi.org/10.1016/j.electacta.2021.139050.
[29] F. Arduini, F. Di Nardo, A. Amine, L. Micheli, G. Palleschi, D. Moscone, Carbon Black-Modified Screen-Printed Electrodes as Electroanalytical Tools, Electroanalysis 24 (2012) 743–751, https://doi.org/10.1002/elan.201100561.
[30] A.P.S. Chauhan, K. Chawla, Comparative studies on graphite and carbon black powders, and their dispersions, J. Mol. Liq. 221 (2016) 292–297, https://doi.org/10.1016/j.molliq.2016.05.043.
[31] K. Toko, Y. Tahara, M. Habara, H. Ikezaki, Potentiometric electronic tongue using lipid/polymer membrane, in: Electronic Tongues, IOP Publishing, 2021, https://doi.org/10.1088/978-0-7503-3687-1ch2.
[32] M.Y. Kim, J.W. Lee, D.J. Park, J.Y. Lee, N.V. Myung, S.H. Kwon, K.H. Lee, Highly stable potentiometric sensor with reduced graphene oxide aerogel as a solid contact for detection of nitrate and calcium ions, J. Electroanal. Chem. 897 (2021), https://doi.org/10.1016/j.jelechem.2021.115553.
[33] M. He, Y. Li, X. Yu, H. Yang, A nitrate ion-selective electrode based on tetradodecylammonium bromide, Sens Lett. 13 (2015) 986–991, https://doi.org/10.1166/sl.2015.3567.
[34] X. Wu, Y. Tahara, R. Yatabe, K. Toko, Taste Sensor: Electronic Tongue with Lipid Membranes, Anal. Sci. 36 (2020) 147–159, https://doi.org/10.2116/analsci.19R008.
[35] F.C. Vicentini, P.A. Raymundo-Pereira, B.C. Janegitz, S.A.S. Machado, O. Fatibello-Filho, Nanostructured carbon black for simultaneous sensing in biological fluids, Sens Actuators B Chem. 227 (2016) 610–618, https://doi.org/10.1016/j.snb.2015.12.094.
[36] Y. Lyu, S. Gan, Y. Bao, L. Zhong, J. Xu, W. Wang, Z. Liu, Y. Ma, G. Yang, L. Niu, Solid-contact ion-selective electrodes: response mechanisms, transducer materials and wearable sensors, Membr. (Basel) 10 (2020) 1–24, https://doi.org/10.3390/membranes10060128.
[37] M.A. Rashed, M. Faisal, M. Alsaiari, S.A. Alsareii, F.A. Harraz, MWCNt-doped polypyrrole-carbon black modified glassy carbon electrode for efficient electrochemical sensing of nitrite ions, Electrocatalysis 12 (2021) 650–666, https://doi.org/10.1007/s12678-021-00675-6.
[38] V. Mazzaracchio, A. Serani, L. Fiore, D. Moscone, F. Arduini, All-solid state ion-selective carbon black-modified printed electrode for sodium detection in sweat, Electro Acta 394 (2021), 139050, https://doi.org/10.1016/j.electacta.2021.139050.
[39] T. Ozer, C.S. Henry, All-solid-state potassium-selective sensor based on carbon black modified thermoplastic electrode, Electro Acta 404 (2022), 139762, https://doi.org/10.1016/j.electacta.2021.139762.
[40] G.A. Crespo, S. Macho, F.X. Rius, Ion-selective electrodes using carbon nanotubes as ion-to-electron transducers, Anal. Chem. 80 (2008) 1316–1322, https://doi.org/10.1021/ac071156l.
[41] J. Ye, F. Li, S. Gan, Y. Jiang, Q. An, Q. Zhang, L. Niu, Using sp2-C dominant porous carbon sub-micrometer spheres as solid transducers in ion-selective electrodes, Electrochem Commun. 50 (2015) 60–63, https://doi.org/10.1016/j.elecom.2014.10.014.
[42] D. Chai, Y. Sun, Z. Li, H. Yang, S. Mao, J. Tang, W. Gong, X. Zeng, A novel inorganic redox buffer of r-GO/Ag@AgCl/TMMCl utilized as an effective ion-to-electron transducer for a solid contact calcium ion-selective electrode, Sens Actuators B Chem. 367 (2022), 132055, https://doi.org/10.1016/j.snb.2022.132055.
[43] D. Chai, Y. Sun, Z. Li, H. Yang, S. Mao, J. Tang, W. Gong, X. Zeng, A novel inorganic redox buffer of r-GO/Ag@AgCl/TMMCl utilized as an effective ion-to-electron transducer for a solid contact calcium ion-selective electrode, Sens Actuators B Chem. 367 (2022), https://doi.org/10.1016/j.snb.2022.132055.
[44] M.Y. Kim, J.W. Lee, D.J. Park, J.Y. Lee, N.V. Myung, S.H. Kwon, K.H. Lee, Highly stable potentiometric sensor with reduced graphene oxide aerogel as a solid contact for detection of nitrate and calcium ions, J. Electroanal. Chem. 897 (2021), https://doi.org/10.1016/j.jelechem.2021.115553.
[45] T. Ozer, Carbon composite thermoplastic electrodes integrated with mini - printed circuit board for wireless detection of calcium ions, Anal. Sci. (2022), https://doi.org/10.1007/s44211-022-00164-w.
[46] C.Z. Lai, M.A. Fierke, A. Stein, P. Bühlmann, Ion-selective electrodes with three-dimensionally ordered macroporous carbon as the solid contact, Anal. Chem. 79 (2007) 4621–4626, https://doi.org/10.1021/ac070132b.
[47] W. Tang, J. Ping, K. Fan, Y. Wang, X. Luo, Y. Ying, J. Wu, Q. Zhou, All-solid-state nitrate-selective electrode and its application in drinking water, Electro Acta 81 (2012) 186–190, https://doi.org/10.1016/j.electacta.2012.07.073.
[48] L. Zhang, Z. Wei, P. Liu, An all-solid-state NO3- ion-selective electrode with gold nanoparticles solid contact layer and molecularly imprinted polymer membrane, PLoS One 15 (2020), https://doi.org/10.1371/journal.pone.0240173.
[49] C. Jiang, Y. Yao, Y. Cai, J. Ping, All-solid-state potentiometric sensor using single-walled carbon nanohorns as transducer, Sens Actuators B Chem. 283 (2019) 284–289, https://doi.org/10.1016/j.snb.2018.12.040.
[50] K. Toko, Y. Tahara, Beer Analysis Using an Electronic Tongue, Elsevier Inc,, 2016, https://doi.org/10.1016/B978-0-12-800243-8.00016-0.
[51] M. Wang, C. Septier, H. Brignot, C. Martin, F. Canon, G. Feron, Astringency sensitivity to tannic acid: effect of ageing and saliva, Molecules 27 (2022), https://doi.org/10.3390/molecules27051617.
[52] Y. Li, Y. Yang, Y. Jiang, S. Han, Detection of tannic acid exploiting carbon dots enhanced hydrogen peroxide/potassium ferricyanide chemiluminescence, Microchem. J. 157 (2020), https://doi.org/10.1016/j.microc.2020.105113.
[53] S.T. Palisoc, E.J.F. Cansino, I.M.O. Dy, C.F.A. Razal, K.C.N. Reyes, L.R. Racines, M. T. Natividad, Electrochemical determination of tannic acid using graphite electrodes sourced from waste zinc-carbon batteries, Sens Biosensing Res 28 (2020), https://doi.org/10.1016/j.sbsr.2020.100326.
[54] S. Sterneder, V. Stoeger, C.A. Dugulin, K.I. Liszt, A. Di Pizio, K. Korntheuer, A. Dunkel, R. Eder, J.P. Ley, V. Somoza, Astringent gallic acid in red wine regulates mechanisms of gastric acid secretion via activation of bitter taste sensing receptor TAS2R4, J. Agric. Food Chem. 69 (2021) 10550–10561, https://doi.org/10.1021/acs.jafc.1c03061.
[55] Y. Harada, Y. Tahara, K. Toko, Study of the relationship between taste sensor response and the amount of epigallocatechin gallate adsorbed onto a lipid-polymer membrane, Sensors 15 (2015) 6241–6249, https://doi.org/10.3390/s150306241.
[56] N. Hayashi, T. Ujihara, S. Jin, Detection of catechins using a fluorescent molecule and its application toward the evaluation of astringent intensity, Analyst (2022), https://doi.org/10.1039/d2an00990k.
[57] N. Hayashi, R. Chen, H. Ikezaki, S. Yamaguchi, D. Maruyama, Y. Yamaguchi, T. Ujihara, K. Kohata, Techniques for Universal Evaluation of Astringency of Green Tea Infusion by the Use of a Taste Sensor System, Biosci. Biotechnol. Biochem 70 (2006) 626–631, https://doi.org/10.1271/bbb.70.626.
[58] M. Narukawa, H. Kimata, C. Noga, T. Watanabe, Taste characterisation of green tea catechins, Int J. Food Sci. Technol. 45 (2010) 1579–1585, https://doi.org/10.1111/j.1365-2621.2010.02304.x.
[59] J. Yeom, A. Choe, S. Lim, Y. Lee, S. Na, H. Ko, Soft and ion-conducting hydrogel artificial tongue for astringency perception, Sci. Adv. 6 (2020) 1–8, https://doi.org/10.1126/sciadv.aba5785.
[60] S. Ma, H. Lee, Y. Liang, F. Zhou, Astringent mouthfeel as a consequence of lubrication failure, Angew. Chem. Int. Ed. 55 (2016) 5793–5797, https://doi.org/10.1002/anie.201601667.

Moch. Rifqi Tamara received his B.Sc. degree in physics from Sriwijaya University Indonesia in 2017. He received PMDSU scholarship from the Ministry of Education, Culture, Research, and Technology of the Republic of Indonesia and currently is a Ph.D. student in Physics Department, Universitas Gadjah Mada. His current research interest includes instrumentation, machine learning, and taste sensor system.

Danang Lelono received his B.Sc. degree in Electronics and Instrumentations from Universitas Gadjah Mada Indonesia in 1995, M.T. degree in applied Electronics from Universitas Gadjah Mada Indonesia in 2003, and Doctor degree in Physics from the Universitas Gadjah Mada Indonesia in 2017. Currently, he was appointed as an assistant professor in Electronics and Instrumentation in 2020. His current research interests are mainly sensor and sensor systems, embedded systems, and smart instruments. He has published more than 50 peer-reviewed papers.

Roto Roto received his B.Sc. degree in chemistry from Universitas Gadjah Mada Indonesia in 1991, M.Sc. degree in applied chemistry from Keio University Japan in 1998, and Ph.D. degree in chemistry from the University of New Brunswick Canada in 2005. He was appointed as an associate professor in chemistry in 2007 and is currently a professor in chemistry at the Department of Chemistry Universitas Gadjah Mada Indonesia. His current research interests are mainly surface electrochemistry, layered materials, and sensing of chemicals including volatile organic compounds and gases. He has published more than 100 peer-reviewed papers.

Kuwat Triyana received his B.Sc. degree in physics from Universitas Gadjah Mada, Indonesia in 1991, his M.Sc. degree in applied physics from Institut Teknologi Bandung, Indonesia in 1997, and his Doctor of Engineering degree in Applied Science for Electronics and Materials from the Kyushu University Japan in 2004. He was appointed as an associate professor in physics in 2008 and is currently a professor in physics at the Department of Physics Universitas Gadjah Mada Indonesia. Currently, he is a President of Material Research Society of Indonesia (MRS-id) and a founder of start-up company of PT. Nanosense Instrument Indonesia. His current research interests are mainly sensor and sensor systems of electronic tongue and electronic nose, quartz crystal microbalance-based chemosensors, and nanofibers. He has published more than 150 peer-reviewed papers.